Structure, Vol. 12, 65–74, January, 2004, ©2004 Elsevier Science Ltd. All rights reserved. DOI 10.1016/j.str.2003.11.017

Molecular Basis of Proton Blockage in Aquaporins

Nilmadhab Chakrabarti,[1,2] Emad Tajkhorshid,[3] Benoît Roux,[4] and Régis Pomès[1,2,*]
[1]Structural Biology and Biochemistry
Hospital for Sick Children
555 University Avenue
Toronto, Ontario M5G 1X8
Canada
[2]Department of Biochemistry
University of Toronto
Toronto, Ontario
Canada
[3]Theoretical and Computational Biophysics Group
Beckman Institute
University of Illinois at Urbana-Champaign
405 North Mathews
Urbana, Illinois 61801
[4]Department of Biochemistry
Weill Medical College of Cornell University
1300 York Avenue
New York, New York 10021

Summary

Water transport channels in membrane proteins of the aquaporin superfamily are impermeable to ions, including H^+ and OH^-. We examine the molecular basis for the blockage of proton translocation through the single-file water chain in the pore of a bacterial aquaporin, GlpF. We compute the reversible thermodynamic work for the two complementary steps of the Grotthuss "hop-and-turn" relay mechanism: consecutive transfers of H^+ along the hydrogen-bonded chain (hop) and conformational reorganization of the chain (turn). In the absence of H^+, the strong preference for the bipolar orientation of water around the two Asn-Pro-Ala (NPA) motifs lining the pore over both unidirectional polarization states of the chain precludes the reorganization of the hydrogen-bonded network. Inversely, translocation of an excess proton in either direction is opposed by a free-energy barrier centered at the NPA region. Both hop and turn steps of proton translocation are opposed by the electrostatic field of the channel.

Introduction

Aquaporins (AQPs) are membrane water channels present in all life forms, and more than 100 of them have been characterized (Agre et al., 1998; Borgnia et al., 1999) since their discovery more than a decade ago. Aquaporin-1 was first identified as an integral membrane protein in red blood cells and renal proximal tubules (Denker et al., 1988, Preston and Agre, 1991), where it functions as a water-selective membrane pore (Preston et al., 1992). Eleven human AQPs have been identified, and their impaired function may lead to pathological situations, such as nephrogenic diabetes insipidus and congenital cataract of the eye (Borgnia et al., 1999; Kozono et al., 2002). All members of the AQP superfamily act as passive transporters of water. Aquaglyceroporins, a subfamily of AQPs, have the ability to conduct small, linear polyols stereoselectively in addition to water molecules (Fu et al., 2000; Borgnia et al., 1999; Jensen et al., 2002; Unger, 2000). The most studied aquaglyceroporin is the *E. coli* glycerol uptake facilitator GlpF, a channel used by organisms to absorb glycerol from the environment for use in metabolism when there is little glycerol available.

Atomic resolution models of human aquaporin-1 (AQP1) based on electron microscopy revealed the tetrameric architecture and folding of AQPs (Murata et al., 2000; Ren et al., 2001). GlpF was the first AQP whose high-resolution X-ray crystallographic structure (2.2 Å) was determined (Fu et al., 2000). GlpF and AQP1 exhibit a remarkable structural similarity (Unger, 2000). The first GlpF structure included three glycerol molecules, a natural substrate for GlpF, in each monomer. Molecular dynamics (MD) simulation of glycerol-saturated GlpF shed light into the details of protein-substrate interaction and conduction pathway (Jensen et al., 2001). In each monomer, the transmembrane segment of the channel is formed by six helices and two half-membrane spanning loops that meet each other at the center of the channel. These two loops are related by quasi 2-fold symmetry and are structurally and functionally important (Murata et al., 2000; Fu et al., 2000; Ren et al., 2001; Zhu et al., 2001; Jensen et al., 2001; Sui et al., 2001). Half of each loop is nonhelical and defines a curvilinear conduction pathway constituted by backbone carbonyl groups that are exposed into the channel interior (Jensen et al., 2001). The other half of each loop (known as M3 and M7 in GlpF, HB and HE in AQP1) is α helical. These helices terminate at the channel center, where two conserved NPA (Asn-Pro-Ala) motifs meet each other (Fu et al., 2000; Murata et al., 2000; Sui et al., 2001). Internal hydrogen bonds within the NPA motifs lead to a configuration in which one of the amide hydrogen atoms of each asparagine points toward the pore. Together, these two NH_2 groups provide two hydrogen-bonding sites for the permeants at the center of the channel. Three-dimensional structures of the glycerol-free GlpF channel have also been solved by X-ray crystallography (Tajkhorshid et al., 2002), revealing the presence of a single file of water molecules. Recent MD studies have addressed the molecular mechanism of water transport in AQP1 and GlpF (de Groot and Grubmüller, 2001; Tajkhorshid et al., 2002; Zhu et al., 2002; Jensen et al., 2003).

AQPs transport water efficiently, but they are impermeable to charged species. Such selectivity is of crucial importance to the proper function of cell membranes, as the flow of water in response to osmotic stress must not disturb the electrochemical properties of the membrane. Blockage of protons is essential in maintaining

*Correspondence: pomes@sickkids.ca

the transmembrane proton gradient in the cell (Mitchell, 1961). However, this property is somewhat unexpected given the presence of a chain of water molecules in the pore. Water chains embedded in biological channels are known to mediate the long-range movement of H^+ via a hop-and-turn Grotthuss relay mechanism (de Grotthuss, 1806; Nagle and Morowitz, 1978; Agmon 1995; Pomès and Roux, 1996, 1998, 2002). In this process of structural diffusion, the excess proton need not diffuse through the pore. Instead, successive transfers (hops) exchange hydrogen nuclei along hydrogen bonds forming an extended network (proton wire); because this process inverts the polarity of proton-relaying groups, proton hopping is complemented by the reorientation (turn) of each group in the chain (Pomès and Roux, 1998, 2002). Together, these two steps, which correspond respectively to the propagation of an ionic and a bonding defect, result in the long-range displacement of H^+ in proteins (Nagle and Morowitz, 1978; Pomès and Roux, 1996). Detailed theoretical studies of water wires embedded in native and chemically modified forms of the gramicidin channel have uncovered the balance of factors at play in the molecular mechanism of proton translocation (Pomès and Roux, 1996, 2002; Yu and Pomès, 2003). In particular, these studies have shown how structural fluctuations of the hydrogen-bonded network formed by the water chain and the channel mediate the rapid, passive transport of H^+.

In the present work, we study the properties of the hydrogen-bonded network in the single-file region of AQPs in order to determine the molecular basis for the exclusion of protons. Previous studies of the water conduction pathway have been used to infer two possible mechanisms of proton blockage, respectively by control of the orientation of the water chain and by interruption of the connectivity of the hydrogen-bonded network. MD simulations have shown that permeating water molecules adopt a preferential orientation in the single-file region of the GlpF pore (Tajkhorshid et al., 2002). One water molecule accepts two hydrogen bonds from the two NPA motifs and orients perpendicularly to the channel axis, and the water molecules on either side form polarized hydrogen-bonded chains extending in opposite directions (Tajkhorshid et al., 2002). This bipolar organization was ascribed to the opposed dipoles of the M3 and M7 helices (Murata et al., 2000; Tajkhorshid et al., 2002) as well as to hydrogen-bond donation by the NPA motifs (Tajkhorshid et al., 2002). Because the bipolar arrangement, with OH bonds pointing outwards, is incompatible with the uptake of an excess proton into the pore from either end, it was proposed that proton blockage results from orientational control (Tajkhorshid et al., 2002). De Groot et al. (2001) postulated that proton exclusion arises from the disruption of the single-file water chain in the narrowest part of the pore, which is formed by an arginine and by two aromatic residues at the periplasmic mouth. However, the translocation of a bonding defect has not been considered, and neither of these two postulates has been tested in the presence of an excess proton in the lumen.

To gain a better understanding of the thermodynamic basis of proton exclusion in AQPs, we use molecular simulations to examine the structural fluctuations of the hydrogen-bonded network in the single-file region of the GlpF channel successively with and without an excess proton. The reversible work for the turn step of structural diffusion is computed by modulating the arrangement of water dipoles in the GlpF pore in the absence of an excess proton. We then characterize the hop step of the Grotthuss mechanism by computing the potential of mean-force for forcing an excess proton through the GlpF pore. Analysis of the free energy profiles for the translocation of bonding and ionic defects in the water chain indicates that proton blockage is essentially achieved by the electrostatic field of the channel.

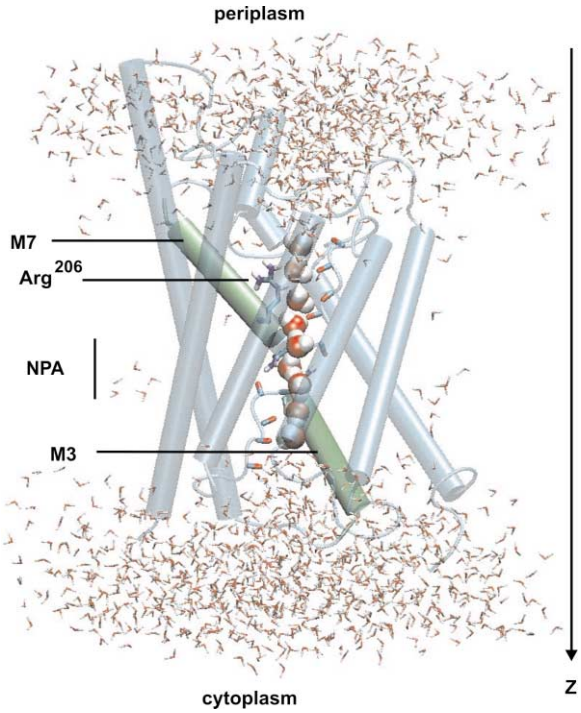

Figure 1. The Molecular System Simulated in the Present Study

The monomeric GlpF channel is shown in α-carbon trace. Water molecules on either side of the pore are shown, and the nine water molecules in the 20 Å long single-file pore ($-6 \leq z \leq 14$ Å) are highlighted in space-filling representation. Also highlighted are salient features of the lumen: Arg206 at the selectivity filter in the periplasmic entry, the two Asn side chains of the conserved NPA motifs, carbonyl groups protruding into the pore, and α helices M3 and M7. This and the following depictions of molecular structures were generated with the VMD program (Humphrey et al., 1996).

Results

The simulated molecular system is shown in Figure 1. The 20 Å long constriction region of the GlpF monomer accommodates nine water molecules in single-file arrangement. Hydrogen-bonding partners of these water molecules include the backbone carbonyl groups (C=O) of residues 64–67 and 199–202, which protrude into the channel. The other hydrogen-bonding groups lining the channel consist of the positively charged residue Arg206, near the periplasmic mouth, and the two conserved asparagines (Asn68 and Asn203) of the NPA motifs (Murata et al., 2000; Fu et al., 2000; Sui et al., 2001;

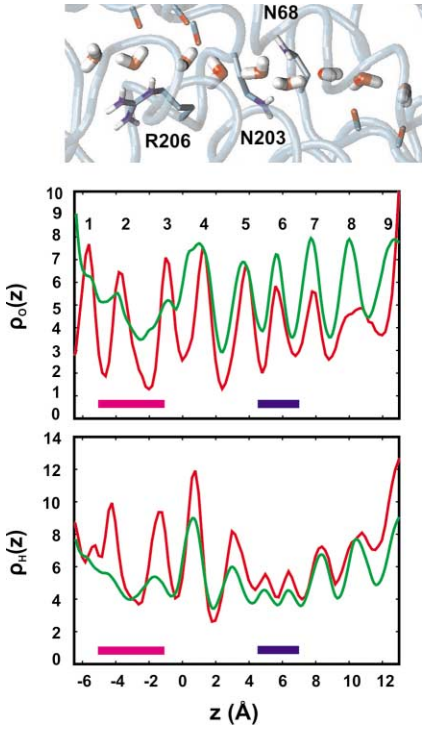

Figure 2. Equilibrium Distribution of Oxygen and Hydrogen Atoms of the Single-File Chain of Water Molecules in the Channel Pore

The results obtained in the present study (red) are compared with the results obtained from a simulation by Tajkhorshid et al. (2002) (green). Top: representative conformation of the nine water molecules in the single file, shown with their hydrogen-bonding partners lining the channel; middle: relative atomic density of oxygens, $\rho_O(z)$; bottom: relative atomic density of hydrogens, $\rho_H(z)$. In this and subsequent figures, the location of the selectivity filter ($-5 \leq z \leq -1$ Å) and of the NPA motifs ($4.75 \leq z \leq 7$ Å) are indicated by pink and blue bars, respectively.

Nollert et al., 2001). Together with Arg206, two aromatic residues (Trp48 and Phe200) form the selectivity filter. This bottleneck has been proposed to work as a size-exclusion filter and was observed to disrupt the hydrogen-bonded water chain (de Groot et al., 2001). The other groups lining the channel (data not shown) are hydrophobic. The amphipathic nature of the pore along the conduction pathway is of crucial importance to the orientational control of water and glycerol permeants in the lumen (Tajkhorshid et al., 2002). Two half helices, M3 and M7, were shown to contribute to the bipolar orientation of the water chain around the NPA region (Tajkhorshid et al., 2002).

The structure and fluctuations of the water chain obtained in the absence of an excess proton confirm the results of previous simulation studies. The equilibrium distribution of the nine single-file water molecules is shown in Figure 2. The top panel depicts the preferred orientation of the water chain, whereas the middle and bottom panels show the distribution of oxygen and hydrogen atoms, respectively. Overall, the results computed from a 2 ns simulation with the present model are in good agreement with those reported from a simulation of the channel tetramer in a lipid membrane (Tajkhorshid et al., 2002). Both O and H distributions obtained from our finite-size model reproduce the preferred localization of water atoms obtained by Tajkhorshid et al. (2002). These preferred positions result from hydrogen bonding with the channel. Protruding carbonyl groups stabilize permeating water molecules along the conduction pathway. The amide groups of Asn68 and Asn203 donate one hydrogen bond each to the sixth water molecule from the periplasm. The bipolar orientation of water molecules identified in previous studies (Tajkhorshid et al., 2002; de Groot and Grubmüller 2001) is reflected in the relative arrangement of O and H atoms. In particular, the symmetric distribution of two H atoms around $z \sim 6$ Å confirms that water 6 remains oriented perpendicular to the channel. Dynamic fluctuations are in very good agreement except in the region of the selectivity filter. In both simulations, a gap in O peaks 2 and 3 at $z \sim -2$ Å points to a resilient interruption in the hydrogen-bonded water chain. However, water molecules near the periplasmic end of the pore are somewhat less mobile in the present simulations, which reflects the fact that no net permeation of water was allowed by construction. The distribution of O atoms obtained in the absence of restraints (Tajkhorshid et al., 2002) suggests that water permeation gives rise to the occasional migration of this hydrogen-bonding defect.

The potential of mean force (PMF) for the turn step of the Grotthuss mechanism is depicted in Figure 3 together with three representative snapshots of the water chain. The PMF profiles computed successively with the TIP3P and PM6 force fields of water are in very good qualitative and quantitative agreement with each other despite fundamental differences between the two water models. The free energy profile for the reorientation of water dipoles in the pore indicates that the preference for the bipolar organization of the water chain is very strong. At $\mu_z \sim -1$ e·Å, the bipolar conformation (B) is overwhelmingly favored over the two metastable states of the chain, A and C (respectively at $\mu_z = -8$ and 8 e·Å). The latter two conformers correspond to fully polarized chains, with water dipole moments pointing respectively toward the periplasmic and cytoplasmic vestibules. The free energy barrier to move the bonding defect from water 6 to the periplasm (B→C transition) is 12–16 kcal/mol with PM6 and TIP3P water models, whereas that for migration to the cytoplasmic vestibule (B→A transition) is 7–8 kcal/mol. These two translocation processes correspond to the reorientation of water molecules 1–6 and 6–9, respectively.

The PMF for the translocation of an excess proton (hop) is depicted in Figure 4. The top four panels illustrate representative configurations of the protonated water chain as H^+ is forced from the periplasmic mouth of the channel toward the cytoplasmic mouth. The free energy profile consists of a barrier that starts at $\xi = -2$ Å and peaks to 4.5 kcal/mol at the NPA site ($\xi = 6$ Å). The corresponding snapshot (configuration III) shows that, among all nine single-file water molecules, water 6 is least likely to host the excess proton. Accordingly, water molecules 4–7 are pulled close to each other, reflecting the relative delocalization of the excess proton in the NPA region. This may be due in part to the lack of hydrogen-bond acceptors at the NPA site, which makes

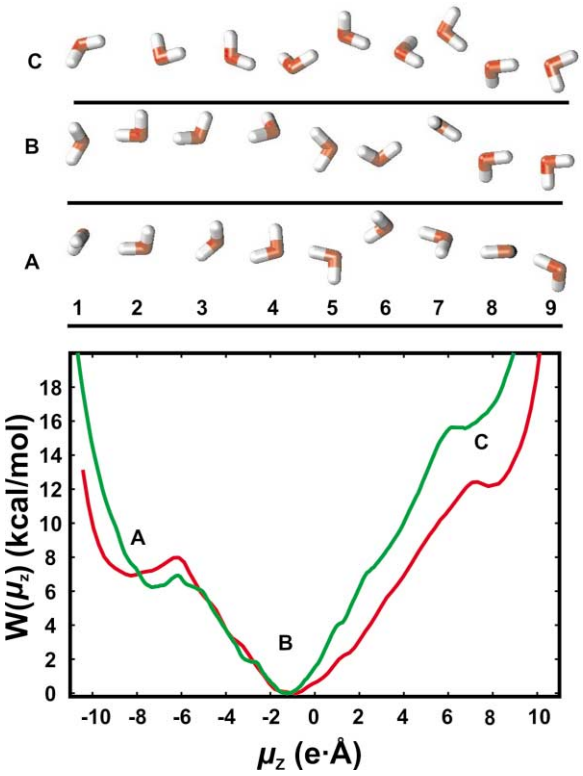

Figure 3. Preferential Organization of the Water Chain in the Absence of an Excess Proton

(Top) Three representative conformations of the hydrogen-bonded water chain in the GlpF pore. (A) Fully-polarized water chain with OH bonds oriented toward the periplasmic entry ($\mu_z = -8$ e·Å); (B) preferred bipolar arrangement of the water chain ($\mu_z = -1$e·Å), with a bonding defect on water 6 at the NPA site; (C) fully-polarized water chain with OH bonds oriented toward the cytoplasmic entry ($\mu_z =$ 7.5 e·Å). (Bottom) Potential of mean force (PMF) for the reorientation of the single-file water chain obtained with water models TIP3P (green) and PM6 (red). The primary minimum corresponds to conformation B and the two secondary minima to conformations A and C. In the case of the TIP3P model, μ_z was scaled by a factor of 0.417, the fractional charge of H atoms in that potential (Jorgensen et al., 1983), for consistency with the magnitude of μ_z obtained with the PM6 model, in which the formal charge of hydrogen is 1.

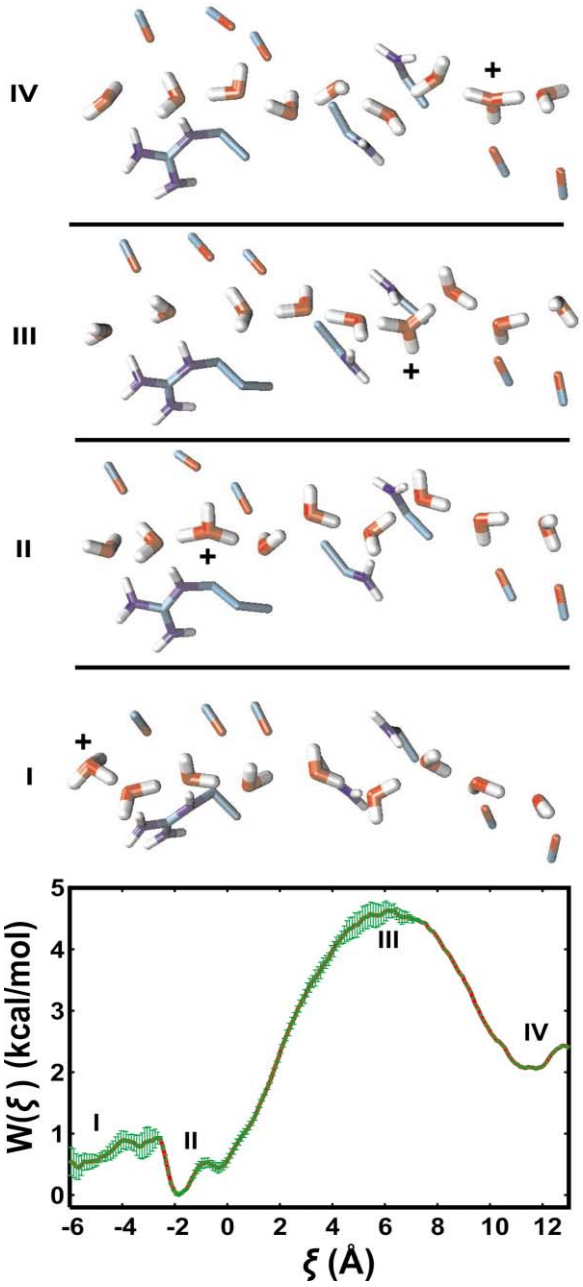

Figure 4. Structure and Energy of the Protonated Water Chain

(Top) Representative conformations of the protonated water chain in the GlpF pore, with the excess proton (I) around Arg206 at the periplasmic mouth, (II) between the selectivity filter and the NPA region, (III) around NPA region, and (IV) at the cytoplasmic mouth. (Bottom) Potential of mean force (PMF) for the translocation of an excess proton through the single-file chain of water molecules. The free energy barrier peaks at the NPA site.

these water molecules relatively unfavorable proton hosts (Pomès and Roux, 2002). The relative flatness of the 2.5 Å wide barrier top may also reflect the delocalization of the excess proton. The proton translocation free energy profile is also essentially flat in the region of the selectivity filter $-6 \leq \xi \leq 0$ Å). Thus, the proximity of positively charged Arg206 does not oppose proton translocation. Snapshots I and II, at $\xi = -5.5$ and -2 Å, correspond to the excess proton hosted respectively by water molecules 1 and 3, on either side of the selectivity filter. Conformer IV, with the excess proton on water 8, lies 2.5 kcal/mol below the barrier top. In both conformations II and IV, the water molecule hosting H^+ is coordinated by three hydrogen-bond acceptors, two from neighboring single-file water molecules and one from a protruding channel carbonyl group (of Phe200 and His66, respectively), mimicking the optimal solvation of protonated water observed in bulk water (Agmon, 1995; Tuckerman et al., 1995) and in the gramicidin channel (Pomès and Roux, 1996, 2002). Throughout the translocation process, the polarization of all water molecules in the chain is dictated by the location of the excess proton, with water dipoles pointing away from the center of charge. Thus, when the excess proton is at the edge of the constriction pore, the water chain is polarized, similar to conformations A and C (see Figure 3) of the

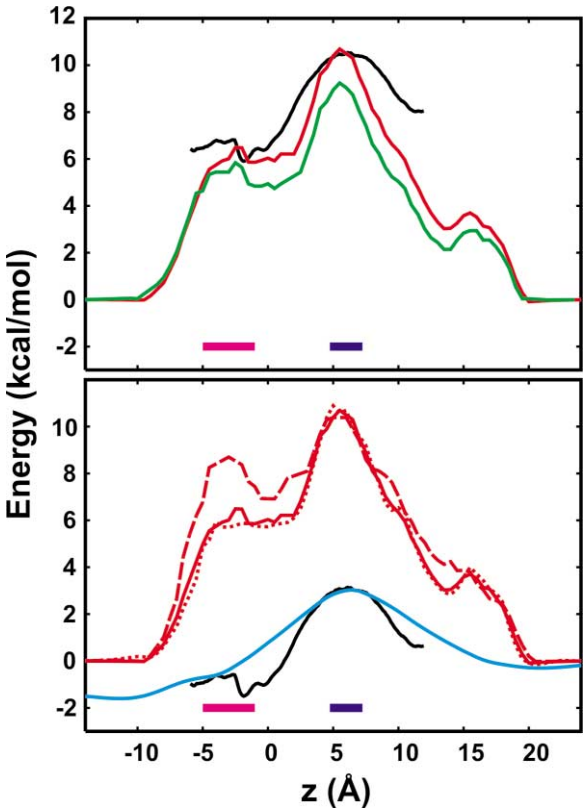

Figure 5. Electrostatic Energy Profiles

(Top) Electrostatic potential energy (ESP) for the movement of a probe cation (with a radius of 1.66 Å) along the GlpF channel (red) shown with the same profile obtained without the low-dielectric membrane environment (green) and with the PMF for the transfer of an excess proton (black) in the single-file region (see Figure 4). The PMF profile was shifted for comparison. (Bottom) Effect of the ionic probe radius on the ESP profile. The three red curves show total ESP profiles obtained with r = 1.66 Å (solid), 1.4 Å (dotted), and 2.03 Å (dashed). The static field contribution to the ESP is shown in blue, and the PMF is again shown in black and shifted for comparison.

unprotonated water chain; with H^+ on water 6, the bipolar orientation of water molecules 1–5 and 7–9 is identical to that of conformation B.

To gauge the effect of the electrostatic field on the translocation of cations throughout the channel, we computed the electrostatic potential (ESP) energy profile for the movement of a cationic probe along the pore in the continuum limit of the solvent (Figure 5). The Born radius of this ion (1.66 Å) was chosen based on the hydration free energy of hydronium (see Experimental Procedures). The ESP profile consists of a 11 kcal/mol barrier centered at the NPA site (z = 5.5 Å) and drops off on both sides of the narrow pore, reaching zero at $z = -12$ and 24 Å. Neglect of the low-dielectric membrane environment results in a 2 kcal/mol downshift of the barrier but does not alter the shape of the ESP. In the single-file region, the ESP for the movement of a positive charge is similar to the PMF for the transfer of an excess proton. Both profiles peak at the same location and feature a shoulder at the selectivity filter, about 4 kcal/mol below the barrier top (Figure 5, top). The static field contribution to the ESP for the translocation of a (point) charge through the pore also exhibits these two features (Figure 5, bottom). Although the total electrostatic barrier is dominated by effects arising from dielectric boundaries (reaction field), the agreement between PMF, ESP, and static field profiles indicates that the free energy for the movement of H^+ in the single-file region is essentially determined by the distribution of charge of the channel. The continuing drops in total electrostatic energy beyond the single-file region (below $z = -6$ Å and above z = 14 Å) suggest that the electrostatic barrier opposing the passage of a cation in the channel originates well outside the narrow pore region. This barrier is not very sensitive to the size of the ionic probe. The ESP profile is identical for a smaller probe ion (radius of 1.4 Å) and does not change appreciably for a larger ion such as potassium (radius of 2.03 Å), except at the bottleneck formed by the selectivity filter, where dielectric effects due to size exclusion result in the emergence of an additional peak centered at Arg206.

Discussion

Electrostatic Control

We have computed the free energy profiles for both hop and turn steps of the Grotthuss mechanism in the single-file region of the GlpF channel. The two PMF profiles, an asymmetric well for the turn, and an asymmetric barrier for the hop, mirror each other in two important respects. First, both extrema are located at the NPA site. Second, the free energy differences between the NPA site and the pore extremities vary in the same proportion in both PMF profiles. At about 7 kcal/mol, the barrier for the translocation of a bonding defect from NPA to the cytoplasmic end of the pore is roughly half the size of the barrier for migration from NPA to the periplasmic extremity of the single-file region (14 ± 2 kcal/mol). Similarly, the barrier facing proton movement from the cytoplasmic end of the pore to NPA (2.5 kcal/mol) is roughly half the size of that opposing the ionic translocation from the periplasmic end (4.5 kcal/mol). Together, these features strongly suggest that the forces opposing both hop and turn steps of the Grotthuss mechanism have the same physical origin. The overall agreement between the hop PMF and the energy profile obtained from continuum electrostatic calculations (Figure 5) indicates that the free energy profile opposing proton transfer trough the pore is essentially determined by electrostatic forces. Thus, the electrostatic field governs not only the structure and fluctuations of the unprotonated water chain, but also the free energy barrier for an excess proton.

Hierarchy of Physical Interactions

In GlpF, the strong electrostatic field of the channel keeps the excess charge away from the NPA site and forces the unprotonated chain into a bipolar organization. The above results suggest that the following hierarchy of molecular interactions is at play in the control of structural diffusion in the GlpF channel: ion-channel > ion-water > water-channel > water-water. The first two inequalities are demonstrated by an analysis of the PMF

for the transfer of an excess proton. Even though ion-water and water-channel interactions are optimized in configuration III, where the bipolar organization of water provides adequate solvation of the positive charge and satisfies the preferred arrangement of the unprotonated water chain (B), ion-channel interactions make it the least likely conformation of the protonated chain. The precedence of ion-water interactions over water-channel interactions is demonstrated in conformations I and IV, where the intrusion of an excess proton at either end of the single-file region is sufficient to polarize the water chain fully despite the intrinsic preference for bipolar conformation B over A and C in the absence of H^+. Water responds to the ionic charge, whereas the comparatively rigid of the channel does not, so that the ionic PMF is dominated by interactions with the channel. Finally, the third inequality is evidenced by the preference for the bipolar orientation of the unprotonated water chain over the fully polarized conformations, which have been shown to be intrinsically favored over all other states in water chains confined in nonpolar environments (Pomès and Roux, 1998). In summary, these results highlight the plasticity of the hydrogen-bonded water chain and show that the orientational polarization of water molecules responds first to the ionic charge, then to the permanent charge distribution of the channel, and last to fluctuating dipoles (i.e., other water molecules).

Limitations of the Model

The overall agreement between the ESP and PMF profiles lends confidence to the results of both MD simulations and PB calculations, despite the limitations arising from the approximations underlying these two approaches. Approximations in the MD calculations reported here include the use of empirical force fields and the finite size of the model, together with restraints precluding water diffusion and limiting the dynamic part of the system to the close vicinity of the single-file pore. However, the analysis of Figure 2 indicates that our use of conformational restraints and of a finite-size model only has a moderate effect on the structure and fluctuations of the pore contents. In addition, the consistency between the properties of the water chain with the results of an earlier study of the channel tetramer in a hydrated membrane (Tajkhorshid et al., 2002) validates the neglect of lipid and of other monomers in the present study. In further support of our finite-size model, the analysis of a simulation of the tetrameric GlpF in a lipid membrane (Jensen et al., 2003) shows that electrostatic interactions of water molecules in the single-file region with the lipid molecules and the other monomers in the tetramer are negligible. Moreover, limitations inherent to the potential energy function used to describe unprotonated water are mitigated by the agreement between the results obtained with very different force fields (Figures 2 and 3). Thus, our molecular model captures the structure and fluctuations of the water chain despite differences in the size of the model and in the potential energy function. PB calculations are plagued by the neglect of thermal fluctuations and the continuum description of the membrane and of the water solvent. The continuum dielectric approximation has been shown to have severe shortcomings to represent the electrostatic response of hydrogen-bonded water molecules in narrow pores (Roux et al., 2000). Probable mitigating factors in the present case include the relative rigidity of the GlpF channel (Jensen et al., 2001) and the fact that overwhelming features governing ionic blockage, rather than the subtle balance of effects involved in ionic solvation and permeation through ion channels, dominate the present results. PB calculations also suffer from the uncertain choice of dielectric constants for the membrane and the protein interior. The electrostatic gradients obtained with different dielectric representations of the membrane (i.e., $\epsilon_{membrane} = 2$ and 80) are in excellent agreement in the pore region (see Figure 5), showing that the effect of the membrane low dielectric is moderate in the narrow pore. Although this is only a rough estimate, the magnitude of the overall electrostatic barrier (over 10 kcal/mol) would be more than sufficient to block proton transport effectively at physiological pH.

Protons versus Other Ions

The dominance of electrostatic forces suggests that the physical basis for the exclusion of protons may also apply to other cations. However, while electrostatic gradients apply equally, in the first approximation, to ions of like charge, this effect may be expected to be modulated by differences in the fine coordination of ionic species, particularly in single-file environments. Ion channels compensate for the partial dehydration of ions, and harness structural differences in the first hydration shell of ions by mimicking the aqueous coordination of permeating ions in narrow pores. Solvation of the aqueous proton by water molecules involves tricoordination of protonated water molecules in hydronium or Zundel cations by three hydrogen-bond acceptors (Agmon, 1995; Tuckerman et al., 1995). In the gA channel, this very coordination is provided by one backbone carbonyl group and two neighboring water molecules to each water O atom (Pomès and Roux, 1996, 2002). Protruding carbonyl groups of GlpF provide adequate tricoordination to water molecules in much of the single-file region of the pore, whereas hydrogen-bond donation by Arg206 and the two Asn side chains of the NPA motifs compromise the ideal coordination of protonated water. The latter factor probably explains the relative delocalization of the excess proton near the NPA site, but does not appear to contribute significantly to the free energy profile of proton translocation. Thus, based on the present study, local solvation effects seem to play a secondary role in the exclusion of H^+ from the GlpF channel. However, the hydration of alkali metal ions, with a larger number of water molecules in the first hydration shell, is very different from that of protons. For example, eight carbonyl groups stabilize K^+ ions in the narrow selectivity filter of the KcsA potassium channel, providing "surrogate solvation" to the permeating cation (Morais-Cabral et al., 2001). Thus, it is likely that the scarcity of carbonyl groups, together with the absence of other groups suitable to the solvation of a cation in the amphipathic pore, would contribute much more significantly to the relative destabilization of other cations. By the same token, in the case of anions it is likely that adverse

solvation effects would take precedence over the electrostatic potential energy. NH dipoles solvate permeating anions in the ClC chloride channel (Dutzler et al., 2002). In AQPs, only the NH_2 groups of Arg206 and of the two NPA Asn side chains can stabilize anions. Both the scarcity and the alternance of CO and NH_2 groups pointing into the lumen discourage the coordination of anions and cations alike.

Selectivity Filter

It was proposed that interruption of the hydrogen-bonded chain prevents the passage of the excess proton through the selectivity filter of AQPs (de Groot and Grubmüller, 2001). The water distribution obtained by Tajkhorshid et al. (2002), however, suggests that this defect is transient in GlpF, appearing in turn between water molecules 1 and 2, and 2 and 3 (see Figure 2). Our results indicate that chain interruption does not have a significant effect in the presence of an excess proton. Furthermore, the conserved Arg in the selectivity filter constitutes only a shoulder in the electrostatic energy profile at the periplasmic vestibule region of GlpF, and does not oppose proton hopping in the single-file region. The lack of a barrier for proton movement past Arg206 (Figure 4) is somewhat surprising considering the strong coulombic repulsion between two positive charges, but can be related to the contribution of other charged groups of the protein, such as Glu43, Glu152, and Asp207, to the electrostatic field of the protein in this region (Jensen et al., 2003). In fact, neither the transfer of an excess proton nor the preferential polarization of water molecules in the selectivity filter are determined by the charge on Arg206. By itself, the guanidinium group of Arg206 would tend to impose a bimodal orientation to nearby water molecules; in particular, water molecules 3, 4,... would point in the opposite direction to that observed in this and other studies (de Groot and Grubmüller, 2001; Tajkhorshid et al., 2002; Jensen et al., 2003). This shows that the charge-charge repulsion between a cation and Arg206 is more than compensated by the electrostatic gradient culminating in the NPA region, in accord with the analysis of Jensen et al. (2003). Further studies will help clarify the role of specific components of the channel in the control of structural diffusion and ion blockage in general.

Mechanism of Proton Blockage

Because our PMF calculation for the excess proton is confined to the single-file region of the pore, we cannot conclude on the precise magnitude of the overall free energy barrier to proton transfer. Nevertheless, it should be noted that the approach of an excess proton into the narrow pore is opposed by the cost of polarizing the unprotonated water chain, which, as indicated by the turn PMF, is about 14 and 7 kcal/mol for the approach of H^+ from the periplasm and from the cytoplasm, respectively (Figure 3). Thus, the free energy barriers opposing hop and turn steps *each* contribute to the molecular mechanism of exclusion of protons from the channel.

Blockage versus Conduction

The above mechanism contrasts with that obtained for the rapid, passive transport of H^+ in the gramicidin cation channel (Pomès and Roux, 1996, 2002). In its conducting form, gA forms a 24 Å long pore containing a single-file chain of up to eight water molecules. Contrary to that found in AQPs, this water chain mediates the relay of protons very effectively (Akeson and Deamer, 1991; Schumaker et al., 2000). The dipole moments of four indole rings located at each of the two lipid-water interfaces give rise to a moderate electrostatic field which has been proposed to increase the proton affinity of water in the lumen relative to bulk (Gowen et al., 2002). However, this field is not strong enough to overcome the intrinsic preference of the unprotonated water chain for a fully (or nearly fully) polarized state (Pomès and Roux, 1998, 2002). In the absence of H^+, membrane voltage, and strong electrostatic gradients in the gA channel, there is no preference for one polarized conformation over the other. Contrary to GlpF, in gA the structure and fluctuations of the hydrogen-bonded network are governed by the properties of the water wire and modulated by short-range interactions with the channel, both hydrogen bonding, charge-dipole, and dipole-dipole (Yu and Pomès, 2003). Each of the single-file water molecules is a good proton host thanks to the proper coordination by carbonyl groups lining the pore of the gA channel (Pomès and Roux, 2002). Accordingly, the PMF for the translocation of an ionic defect in the pore of gA is nearly flat, with a slight (1 kcal/mol) preference for the middle of the channel (Pomès and Roux, 2002). In addition, hydrogen-bond donation to carbonyl groups assists the translocation of a bonding defect by stabilizing partially oriented conformations of the unprotonated water chain. Thus, gA solvates both ionic and bonding defects (Pomès and Roux, 2002). The sensitivity of the relay mechanism to the charge distribution of the channel, which is evidenced in the present study, was uncovered in a recent study of dioxolane-linked gA, where the movement of proton was shown to be modulated by conformational fluctuations exchanging locally distorted states of the channel on a (ns) time-scale commensurate with proton permeation (Yu and Pomès, 2003). In these distorted states, the dipole moments of two carbonyl groups act as conformational switches modifying the preferred organization of the unprotonated chain and confining the excess proton through dipole-dipole and charge-dipole interactions.

Conclusions

By using a combination of methods comprising umbrella sampling simulations with a polarizable/dissociable model and macroscopic continuum electrostatic calculations, we were able to quantify the energetics of proton transport through GlpF. The detailed picture of structural diffusion and the reversible work for the translocation of ionic and bonding defects provided by the present study clarify the physical basis of proton blockage by AQPs. Tajkhorshid et al. (2002) noted the bipolar organization of the water chain and remarked that the orientation of water molecules is incompatible with the penetration of H^+ into the pore from either side. The present study confirms the stringent control of water orientation but also indicates that, although it participates in the exclusion of H^+ from the pore, the bipolar organization

of the chain does not in itself preclude proton hopping in the single-file region. Rather, both turn and hop steps of structural diffusion are opposed by electrostatic gradients around the NPA site. Together, these two effects conspire to block proton permeation through the channel. In view of the highly conserved features of the narrow pore region (Unger, 2000), it is likely that the electrostatic origin of proton blockage extends to other AQPs. Electrostatic forces were also shown to play an important role in the charge selectivity of the KcsA potassium channel (Roux and MacKinnon, 1999) and to modulate the Grotthuss relay mechanism in chemically modified variants of the gramicidin channel (Yu and Pomès, 2003). Although further studies will help clarify the structural origin of permeant selectivity, this work provides meaningful insight into the physical basis for the control of H^+ transport in membrane proteins, one of the most important reactions in biology.

Experimental Procedures

Molecular Model

The initial conformation of GlpF was taken from a previous simulation study of the homotetrameric channel in a hydrated lipid membrane (Tajkhorshid et al., 2002). One monomer, together with slabs of water molecules nearby, was retained, and the rest of the system was discarded (Figure 1). The monomeric system consists of 3839 protein atoms, 9 water molecules in the pore, and 1383 water molecules in the bulk, for a total of 8315 atoms. The inner core, an orthorhombic region of 30 × 14 × 14 Å^3 and consisting of ~1100 atoms, was allowed to move during the MD simulations; the rest of the system was kept fixed.

The CHARMM force field, version 22 (Brooks et al., 1983; MacKerell et al., 1998), was used to model the protein. Bulk water was represented by the TIP3P force field (Jorgensen et al., 1983) and the nine water molecules in the channel pore were modeled successively with TIP3P and with the PM6 model (Stillinger and David, 1978; Stillinger, 1979; Weber and Stillinger, 1982; Pomès and Roux, 1996, 1998). Both force fields were used in the study of the turn step of the Grotthuss mechanism, whereas the PM6 force field was employed in simulations with an excess proton. PM6 is a polarizable and dissociable model of water that consists of O^{2-} and H^+ moieties. This empirical model has been shown to capture the essential features of the mechanism of H^+ transport in biological proton ducts (Mei et al., 1998; Pomès and Roux, 2002).

Geometric constraints were applied on the single-file chain of nine water molecules and on the bulk water to prevent the entrance or exit of water into or from the single-file region of the pore. Planar restraints were imposed on water molecules at the interface of single file and bulk. To check the consistency of this finite-size model, we computed the distribution of oxygen and hydrogen atoms (ρ_O, ρ_H) of PM6 water molecules from a 2 ns simulation and compared it with earlier results obtained from simulations of the full tetrameric channel immersed in an explicit lipid bilayer with periodic boundary conditions (Tajkhorshid et al., 2002). The finite-size model offers the advantage of computational efficiency as well as allowing the study of structural diffusion in the absence of water permeation.

Molecular Dynamics Simulations

The program CHARMM (Brooks et al., 1983) was employed to generate MD trajectories. The Langevin equations of motion were propagated at 300 K with an integration step of 1 fs and a friction coefficient of 5 ps^{-1} applied to all heavy atoms. Nonbonded interactions were calculated without any cut off.

Water Reorientation

The PMF profiles were computed as follows. The configuration of the molecular system was recorded every 5 fs. The projection of the total dipole moment of the lumen content (water chain) on the z axis (channel axis) was calculated for each configuration at time t as $\mu_z(t) = q_O \Sigma_{Oi} z_{Oi}(t) + q_H \Sigma_{Hj} z_{Hj}(t)$ in units of e·Å, where q_O and q_H are the formal charges of single-file water O and H atoms. For the TIP3P water model, q_O and q_H are −0.834 and 0.417 e, whereas for the PM6 model, q_O and q_H are −2 and 1 e, respectively. This reaction coordinate was used in previous studies of the turn step (Pomès and Roux, 1998, 2002; Yu and Pomès, 2003). The PMF profile was calculated from the equilibrium probability distributions of μ_z obtained from the simulations. A biasing potential energy function was imposed on μ_z to force the reorientation of the unprotonated water chain. Harmonic biasing functions of the form $V_i(\mu_z) = (1/2)\, k_i (\mu_z - \mu_{zi})^2$ were used to carry out this umbrella sampling calculation (Torrie and Valleau, 1974, 1977). For all the windows the harmonic k_i coefficients were set to 20 kcal·mol^{-1}·e^{-2}·Å^{-2}. For the TIP3P water chain, the reference μ_{zi} varied in increments of 0.25 e·Å, from −5.0 to 5.0 e·Å. Each window of the umbrella simulation consisted of 10 ps of equilibration and 40 ps of production run for data collection. In the case of the PM6 water chain, μ_{zi} varied in increments of 0.25 e·Å from −11.0 to 11.0 e·Å, and the same protocol was used for each of the 89 windows. The PMF profile was computed by unbiasing and combining windows with the weighted histogram analysis method (WHAM) (Kumar et al., 1992; Roux, 1995).

Proton Hopping

We define a new reaction coordinate to follow the displacement of an excess proton along the water chain as follows: $\xi = (\Sigma_{Oi} W_{Oi})^{-1} (\Sigma_{Oi} z_{Oi} W_{Oi})$, where $W_{Oi} = \Sigma_{Hj} f_{sw}(r_{OiHj}) - 2$ is a weighting function, $f_{sw}(r_{OiHj}) = 1/(1 + exp[\{r_{OiHj} - r_{sw}\}/d_{sw}])$ is a switching function, and O_i, H_j are respectively oxygen and hydrogen atoms of the single-file water chain. Based on earlier studies using the PM6 model (Pomès and Roux, 1996), we chose $d_{sw} = 0.05$ Å and $r_{sw} = 1.4$ Å. This continuous and derivable reaction coordinate keeps track of the water molecule(s) that are close to three hydrogen nuclei, yielding the location of the oxygen atom for a hydronium ion OH_3^+ and that of the shared proton in a symmetric Zundel ion $(O_2H_5)^+$. The PMF profile of transfer of an excess proton in the water chain was computed from equilibrium distributions of ξ obtained from umbrella sampling simulations. A biasing potential energy function was imposed on ξ to force the sampling over the entire pore region. 43 successive sampling windows with harmonic biasing functions of the form $V_i(\xi) = (1/2)\, k_i (\xi - \xi_i)^2$ were used, with $k_i = 0.75$ kcal·mol^{-1}Å^{-2} and ξ_i ranging from −6.5 to 14.5 Å in increments of 0.5 Å. Each window of umbrella sampling consisted of 20 ps of equilibration followed by 60 ps of production. The reaction coordinate was recorded every 2 fs. The total simulation time required to build the PMF profile for H^+ translocation was 3.44 ns.

Electrostatic Calculations

We computed the total electrostatic potential (ESP) for the passage of a cation through the GlpFpore by solving the linearized Poisson-Boltzmann (PB) equation. The PBEQ module of CHARMM version 28 was used together with the set of optimized atomic radii for amino acids (Nina et al., 1997). All explicit water molecules were removed from the molecular system. The ESP was computed with a cation placed at successive positions along the channel pore. In the continuum approximation, the total electrostatic free energy of the cation in the pore can be expressed as the sum of contributions from the static field (which reflects the charge distribution of the protein) and from the reaction field (which is governed by the low-dielectric boundaries). The radius of the cation was chosen as that of sodium (Nina et al., 1997) because the hydration free energy of that ion, −98 kcal/mol (Burgess, 1978), is comparable to that of hydronium, −102 (Pearson, 1986) to −104 kcal/mol (Chambers et al., 1996). The linearized PB equation was solved on a cubic grid of 151 cells with a cell width of 1.0 Å, with subsequent focusing using a 0.5 Å cell width. The low-dielectric region of the membrane was represented by a slab perpendicular to the z axis and centered at $z = 5$ Å. The thickness of the membrane slab was chosen as 40 Å based on a previous simulation study (Jensen et al., 2001). The dielectric constants used in these calculations were respectively 2, 2, and 80 for protein, membrane, and water. A high-dielectric constant ($\epsilon = 80$) was assigned to the interior of the pore. No transmembrane voltage was applied. The calculation was repeated with a membrane dielectric constant of 80 to gauge the sensitivity of the results to the description of the membrane. Finally, the calculation was repeated with smaller (1.4 Å) and larger (2.03 Å) cation radii to

gauge the sensitivity of the results to the size of the ionic probe; the latter radius corresponds to a K^+ ion (Nina et al., 1997).

Acknowledgments

We thank Klaus Schulten and Wonpil Im for useful discussions. We gratefully acknowledge the Canadian Institutes of Health Research (operating grant MOP43949) and the Ontario Centre for Genomics Computing for support. R.P. is a CRCP Chairholder.

Received: August 23, 2003
Revised: September 29, 2003
Accepted: October 5, 2003
Published: January 13, 2004

References

Agmon, N. (1995). The Grotthuss mechanism. Chem. Phys. Lett. *224*, 456–462.

Agre, P., Bonhivers, M., and Borgnia, M.J. (1998). The aquaporins, blueprints for cellular plumbing systems. J. Biol. Chem. *273*, 4659–4662.

Akeson, M., and Deamer, D.W. (1991). Proton conductance by the gramicidin water wire. Biophys. J. *60*, 101–109.

Borgnia, M.J., Nielsen, S., Engel, A., and Agre, P. (1999). Cellular and molecular biology of the aquaporin water channels. Annu. Rev. Biochem. *68*, 425–458.

Brooks, B.R., Bruccoleri, R.E., Olafson, B.D., States, D.J., Swaminathan, S., and Karplus, M. (1983). CHARMM: a program for macromolecular energy minimization and dynamics calculations. J. Comput. Chem. *4*, 187–217.

Burgess, J. (1978). Metal Ions in Solution (New York: J. Wiley).

Chambers, C.C., Hawkins, G.D., Cramer, C.J., and Truhlar, D.G. (1996). Model for aqueous solvation based on class IV atomic charges and first solvation shell effects. J. Phys. Chem. *100*, 16385–16398.

Denker, B.M., Smith, B.L., Kuhadja, F.P., and Agre, P. (1988). Identification, purification, and partial characterization of a novel Mr 28,000 integral membrane protein from erythorcytes and renal tubules. J. Biol. Chem. *263*, 15634–15642.

de Groot, B.L., and Grubmüller, H. (2001). Water permeation across biological membranes: mechanism and dynamics of aquaporin-1 and GlpF. Science *294*, 2353–2357.

de Grotthuss, C.J.T. (1806). Mémoire sur la décompostion de l'eau et des corps qu'elle tient en dissolution à l'aide de l'électricité galvanique. Ann. Chim. *58*, 54–74.

Dutzler, R., Campbell, E.B., Cadene, M., Chait, B.T., and Mackinnon, R. (2002). X-ray structure of a ClC chloride channel at 3.0 angstrom reveals the molecular basis of anion selectivity. Nature *415*, 287–294.

Fu, D., Libson, A., Miercke, L.J., Weitzman, C., Nollert, P., Krucinski, J., and Stroud, R.M. (2000). The structure of a glycerol-conducting channel reveals the basis for its selectivity. Science *290*, 481–486.

Gowen, J.A., Markham, J.C., Morrison, S.E., Cross, T.A., Busath, D.D., Mapes, E.J., and Schumaker, M.F. (2002). The role of Trp side chains in tuning single proton conduction through gramicidin channels. Biophys. J. *83*, 880–898.

Humphrey, W., Dalke, A., and Schulten, K. (1996). VMD: visual molecular dynamics. J. Mol. Graph. *14*, 33–38.

Jensen, M.Ø., Tajkhorshid, E., and Schulten, K. (2001). The mechanism of glycerol conduction in Aquaglyceroporins. Structure *9*, 1083–1093.

Jensen, M.Ø., Park, S., Tajkhorshid, E., and Schulten, K. (2002). Energetics of glycerol conduction through aquaglyceroporin GlpF. Proc. Natl. Acad. Sci. USA *99*, 6731–6736.

Jensen, M.Ø., Tajkhorshid, E., and Schulten, K. (2003). Electrostatic tuning of permeation and selectivity in aquaporin water channels. Biophys. J., *85*, 2884–2899.

Jorgensen, W.L., Chandrasekhar, J., Madura, J.D., Impey, R.W., and Klein, M.L. (1983). Comparison of simple potential functions for simulating liquid water. J. Chem. Phys. *79*, 926–935.

Kozono, D., Yasui, M., King, L.S., and Agre, P. (2002). Aquaporin water channels: atomic structure and molecular dynamics meet clinical medicine. J. Clin. Invest. *109*, 1395–1399.

Kumar, S., Bouzida, D., Swendsen, R.H., Kollman, P.A., and Rosenberg, J.M. (1992). The weighted histogram analysis method for free-energy calculations in biomolecules, 1. The Method. J. Comput. Chem. *13*, 1011–1021.

MacKerell, A.D., Jr., Bashford, D., Bellott, M., Dunbrack, R.L., Jr., Evanseck, J.D., Field, M.J., Fischer, S., Gao, J., Guo, H., Ha, S., et al. (1998). All-atom empirical potential for molecular modeling and dynamics studies of proteins. J. Phys. Chem. B *102*, 3586–3616.

Mei, H.S., Tuckerman, M.E., Sagnella, D.E., and Klein, M.L. (1998). Quantum nuclear ab initio molecular dynamics study of water wires. J. Phys. Chem. B *102*, 10446–10458.

Mitchell, P. (1961). Coupling of phosphorylation to electron and hydrogen transfer by a chemi-osmotic type of mechanism. Nature *191*, 144–148.

Morais-Cabral, J.H., Zhou, Y., and Mackinnon, R. (2001). Energetic optimization of ion conduction rate by the K^+ selectivity filter. Nature *414*, 37–42.

Murata, K., Mitsuoka, K., Hirai, T., Walz, T., Agre, P., Heymann, J.B., Engel, A., and Fujiyoshi, Y. (2000). Structural determinants of water permeation through aquaporin-1. Nature *407*, 599–605.

Nagle, J.F., and Morowitz, H.J. (1978). Molecular mechanisms for proton transport in membranes. Proc. Natl. Acad. Sci. USA *75*, 298–302.

Nina, M., Beglov, D., and Roux, B. (1997). Atomic Born radii for continuum electrostatic calculations based on molecular dynamics free energy simulations. J. Phys. Chem. B *101*, 5239–5248.

Nollert, P., Harries, W.E.C., Fu, D., Miercke, L.J., and Stroud, R.M. (2001). Atomic structure of a glycerol channel and implications for substrate permeation in aqua (glycero) porins. FEBS Lett. *504*, 112–117.

Pearson, R.G. (1986). Ionization potentials and electron affinities in aqueous solution. J. Am. Chem. Soc. *108*, 6109–6114.

Pomès, R., and Roux, B. (1996). Structure and dynamics of a proton wire: a theoretical study of H^+ translocation along the single-file water chain in the gramicidin channel. Biophys. J. *71*, 19–39.

Pomès, R., and Roux, B. (1998). Free energy profile for H^+ conduction along hydrogen-bonded chains of water molecules. Biophys. J. *75*, 33–40.

Pomès, R., and Roux, B. (2002). Molecular mechanism of H^+ conduction in the single-file water chain of the gramicidin channel. Biophys. J. *82*, 2304–2316.

Preston, G.M., and Agre, P. (1991). Isolation of the cDNA for erythrocyte integral membrane protein of 28 kilodaltons: member of an ancient channel family. Proc. Natl. Acad. Sci. USA *88*, 11110–11114.

Preston, G.M., Carroll, T.P., Guggino, W.B., and Agre, P. (1992). Appearance of water channels in Xenopus oocytes expressing red cell CHIP28 protein. Science *256*, 385–387.

Ren, G., Reddy, V.S., Cheng, A., Melnyk, P., and Mitra, A.K. (2001). Visualization of a water-selective pore by electron crystallography in vitreous ice. Proc. Natl. Acad. Sci. USA *98*, 1398–1403.

Roux, B. (1995). The calculation of the potential of mean force using computer simulations. Comp. Phys. Commun. *91*, 275–282.

Roux, B., and Mackinnon, R. (1999). The cavity and pore helices in KcsA K^+ channel: electrostatic stabilization of monovalent cations. Science *285*, 100–102.

Roux, B., Bernèche, S., and Im, W. (2000). Ion channels, permeation, and electrostatics: insight into the function of KcsA. Biochemistry *39*, 13295–13306.

Schumaker, M.F., Pomès, R., and Roux, B. (2000). A combined molecular dynamics diffusion model of single proton conduction through gramicidin. Biophys. J. *79*, 2840–2857.

Stillinger, F.H. (1979). Dynamics and ensemble averages for the

polarization models of molecular interactions. J. Chem. Phys. *71*, 1647–1651.

Stillinger, F.H., and David, C.W. (1978). Polarization model for water and its ionic dissociation products. J. Chem. Phys. *69*, 1473–1484.

Sui, H., Han, B.G., Lee, J.K., Walian, P., and Jap, B.K. (2001). Structural basis of water-specific transport through the AQP1 water channel. Nature *414*, 872–878.

Tajkhorshid, E., Nollert, P., Jensen, M., Miercke, L.J.W., O'Connell, J., Stroud, R.M., and Schulten, K. (2002). Control of the selectivity of the aquaporin water channel family by global orientational tuning. Science *296*, 525–530.

Torrie, G.M., and Valleau, J.P. (1974). Monte-Carlo free energy estimates using non-Boltzmann sampling—application to subcritical Lennard-Jones fluid. Chem. Phys. Lett. *28*, 578–581.

Torrie, G.M., and Valleau, J.P. (1977). Non-physical sampling distributions in Monte-Carlo free energy estimation: umbrella sampling. J. Comp. Physiol. *23*, 187–199.

Tuckerman, M., Laasonen, K., Sprik, M., and Parrinello, M. (1995). *Ab initio* molecular dynamics simulation of the solvation and transport of H_3O^+ and OH^- ions in water. J. Phys. Chem. *99*, 5749–5752.

Unger, V.M. (2000). Fraternal twins: AQP and GlpF. Nat. Struct. Biol. *7*, 1082–1084.

Weber, T.A., and Stillinger, F.H. (1982). Reactive collisions of H_3O^+ and OH^- studied with the polarization model. J. Phys. Chem. *8*, 1314–1318.

Yu, C.-H., and Pomès, R. (2003). Functional dynamics of ion channels: modulation of proton movement by conformational switches. J. Am. Chem. Soc., *125*, 13890–13894.

Zhu, F., Tajkhorshid, E., and Schulten, K. (2001). Molecular dynamics study of aquaporin-1 water channel in a lipid bilayer. FEBS Lett. *504*, 212–218.

Zhu, F., Tajkhorshid, E., and Schulten, K. (2002). Pressure-induced water transport in membrane channels studied by molecular dynamics. Biophys. J. *83*, 154–160.